Available online at www.sciencedirect.com
SCIENCE DIRECT®
Journal of the European Ceramic Society 25 (2005) 3413–3425
www.elsevier.com/locate/jeurceramsoc

A phenomenological description of the rate of the aluminum/oxygen reaction in the reaction-bonding of alumina

Jill M. Aaron[a], Helen M. Chan[b], Martin P. Harmer[b], Maytee Abpamano[a], Hugo S. Caram[a,*]

[a] *Department of Chemical Engineering, Lehigh University, Bethlehem, PA 18015, USA*
[b] *Department of Materials Science and Engineering, Lehigh University, Bethlehem, PA 18015, USA*

Received 24 November 2003; received in revised form 23 August 2004
Available online 22 December 2004

Abstract

The isothermal reaction kinetics of aluminum oxidation in loose Al/Al_2O_3 powder was studied in the temperature range 455–555 °C using thermogravimetry. The powder compositions ranged from 30 to 65 vol.% aluminium, with average Al particle sizes in the range 1.4–2.7 μm The oxygen mole fraction was varied between 20 and 100%. It was found that only 70–80% of the aluminum can be oxidized below the melting point of 660 °C. The weight gain curves were well fitted by assuming that the rate of oxidation was first order with respect to the amount of aluminum, which can be oxidized below 660 °C, left in the sample. The reaction rate was observed to be independent of both the partial pressure of oxygen and the aluminum particle size. It was shown that the same kinetics relationship could also be applied to a broad range of experimental oxidation data in the literature, yielding a common value of the Arrhenius constant and activation energy. The kinetic model was successfully applied to the controlled processing of RBAO powder compacts for constant temperature hold and constant reaction rate cases.

Keywords: Al_2O_3; RBAO; Reaction bonding; Al; Oxidation kinetics

1. Introduction

The reaction-bonded aluminum oxide (RBAO) process was developed by the Advanced Ceramics Group of the Technical University of Hamburg-Harburg in Hamburg, Germany.[1] The RBAO process involves heat treating attrition-milled Al/Al_2O_3 or $Al/Al_2O_3/ZrO_2$ powder compacts in an oxidizing atmosphere to produce Al_2O_3-based ceramics.[1–10] RBAO precursor powders are made using 30–80 vol.% aluminum powder, 20–70 vol.% alumina powder, and 0–20 vol.% zirconia powder. The addition of zirconia improves the microstructure and mechanical properties of the final ceramic.[2,3]

The oxidation of aluminum occurring during the RBAO process is given by the reaction

$$4Al + 3O_2 \rightarrow 2Al_2O_3 \quad (1)$$

This reaction is extremely exothermic and results in volume expansion and weight gain. Due to the weight gain, the reaction rate can be determined using themogravimetry (TG).

Reaction behavior of a typical RBAO powder heated in air is shown in Fig. 1. The furnace temperature was increased at 1 °C/min. The weight gain is plotted against the furnace temperature, which may be different from the actual sample temperature. After the initial weight loss, associated with the evaporation of fugitive species, there is a rapid acceleration of the rate of reaction at a furnace temperature of about 450 °C. The reaction rate reaches a maximum in the furnace temperature range of 500–550 °C. Under these conditions, the sample ignites and there are temperature excursions of up to 1000 °C. As the furnace temperature increases above 550 °C

* Corresponding author. Tel.: +1 610 758 4259; fax: +1 610 758 5057.
E-mail address: hsc0@lehigh.edu (H.S. Caram).

0955-2219/$ – see front matter © 2004 Published by Elsevier Ltd.
doi:10.1016/j.jeurceramsoc.2004.09.012

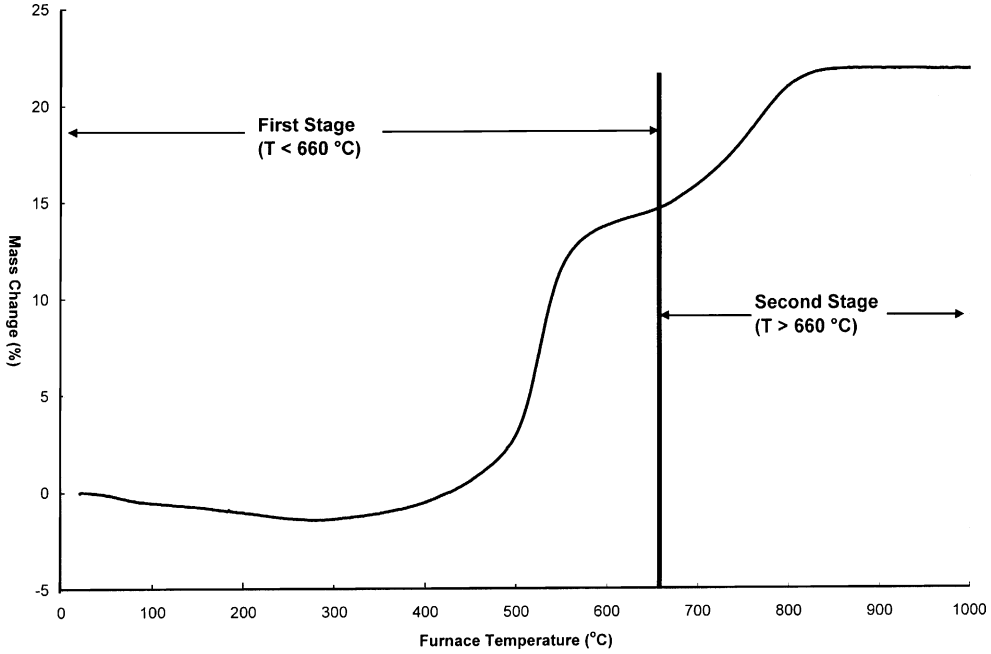

Fig. 1. Reaction behavior of a typical, RBAO powder heated 1 °C/min in air.

the reaction slows down to the point that no further conversion will occur if the furnace temperature does not exceed the melting point of aluminum at 660 °C, when total conversion will occur. It is the uneven volume gains and sharp thermal gradients associated with the ignition phenomena that cause stresses which result in sample cracking.[2–4,6,7] Cracking can be avoided by using low heating rates and isothermal temperature holds that avoid reaction runaway.[2–4,6,7] Knowledge of the reaction kinetics of the oxidation of aluminum can be used to avoid uncontrolled reactions.

The purpose of the present study is to determine the oxidation kinetics of RBAO powders comprising a mixture of Al and Al_2O_3. The oxidation of the Al was studied using thermogravimetry, and kinetic constants were determined as a function of aluminum concentration, oxygen partial pressure, and aluminum particle size. Note that in previous modeling studies, the reaction rate had been assumed to be second order with respect to aluminum, and first order with respect to oxygen, but this had not been confirmed experimentally.[3,6]

As will be seen, the data from the present study yields a kinetic model which, in addition to being directly pertinent to RBAO conversion, has general applicability to studies of Al oxidation in the literature.

2. Background

2.1. Oxidation of aluminum

The oxidation of aluminum has been the subject of many studies.[11–21] Most of them have used thin, flat samples of aluminum, but some work has also been reported in powder samples. The rate of oxidation of aluminum has been observed to be extremely temperature sensitive, and various kinetic models with different mechanisms have been used to describe the oxidation at various temperatures.

Cabrera and Mott[22] developed theories for the mechanisms which control the oxidation of metals for thick, thin, and very thin oxide layers. For thick oxide films and sufficiently high temperatures, either the metal or oxygen ions are soluble in the oxide and diffuse through the oxide layer. The driving force is a concentration gradient that is inversely proportional to the film thickness leading to the classic parabolic rate law of the form

$$X^2 = 2At \tag{2}$$

where t is the time; X, proportional to the amount of aluminum converted and A, a constant proportional to the species diffusivity across the oxide. Since oxygen ions have poor solubility in aluminum oxide, the rate of diffusion of aluminum ions is commonly assumed to control the reaction rate. Thus, the rate of oxidation can be considered to be relatively independent of the oxygen pressure.

Isothermal weight gain experiments below 450 °C resulted in weight gain curves that fit a parabolic rate law.[5,11–13,22] As discussed above this corresponds to the growth of an amorphous oxide layer which is controlled by aluminum ion diffusion through the layer.[14,22] This is also valid for the initial weight gain region above 450 °C, but as will be discussed below the fit does not extend to higher conversions.

An Arrhenius plot of the rate coefficients from data fitting parabolic kinetics below 450 °C and in the initial region

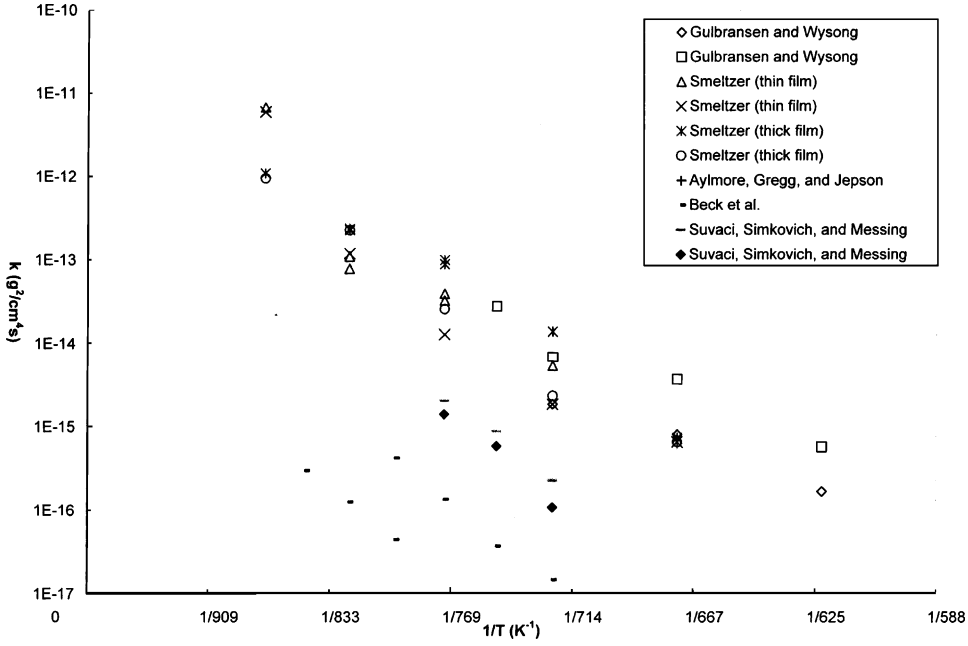

Fig. 2. Arrhenius plot of rate coefficients from data fitting parabolic kinetics from various studies.

above 450 °C for various studies is shown in Fig. 2. Rate coefficient data of Gulbransen and Wysong[11], Smeltzer[15], and Aylmore et al.[13] are closely clustered. Values collected by Beck et al.[17] and Suvaci et al.[18] are significantly lower. Nevertheless, when the data points are considered together, they form a band which suggests a common activation energy. Shown in Table 1 is a wide range of rate constants and activation energies reported by the original authors. The apparent differences disappear when the actual rate coefficients are presented on the same plot. The same phenomenon will be observed with the rate data at higher conversions and temperatures. This is because there are two constants, *k* and E, that can be used to fit the data and many combinations of these two give good fits. Only when the experimental results are plotted together does the similarity between the rates becomes apparent.

At temperatures above 450 °C, and higher conversions, the parabolic model is no longer valid. The observations of an amorphous oxide layer up to about 450 °C with the growth of a crystalline oxide layer at the metal-amorphous oxide interface at higher temperatures indicate that the change from parabolic kinetics is probably due to the nucleation and growth of crystalline alumina.[19,20] This suggests that the second and final regions of the weight gain curves correspond to the nucleation, growth, and cessation of growth of crystalline oxide.[16–18] Oxygen is transported through the amorphous oxide layer to the metal–oxide interface for the formation of crystalline alumina.[20]

Table 1
Activation energies and Arrhenius constants of data fitting parabolic kinetics for various studies

Data source	Temperature range (°C)	Activation energy (kJ/mol)	Arrhenius constant (g^2/cm^4 s)
Gulbransen and Wysong[11]	350–450	96	7.8×10^{-9}
		96	8.4×10^{-7}
Smeltzer[15] (thin film range)	400–600	159	1.6×10^{-3}
		172	8.0×10^{-3}
Smeltzer[15] (thick film range)	400–600	170	1.7×10^{-2}
		212	6.0
Aumann et al.[12]	250–375	48	6.0×10^{-15}
Aumann et al.[12]	375–450	164	2.0×10^{-5}
Beck et al.[17]	450–575	226	7.0×10^{-2}
			5.0×10^{-3}
Suvaci et al.[18]	450–575	206	1.9×10^{-1}
		238	2.4×10^{-1}

3. Experimental procedure

3.1. Powder processing

RBAO powders were prepared from starting powders of Al (spherical powder, 99%+, ∼40 μm, Aldrich Chemical Co. Inc., Milwaukee, WI) and Al_2O_3 (AKP-30, >99.99%, 0.4 μm, Sumitomo Chemical Co. Ltd., Japan). The three powder compositions processed comprised 30, 45, and 65% volume aluminum, with Al_2O_3 as the remaining portion. These compositions will be designated as Al30, Al45, and Al65, respectively. Zirconia, which is often a component of RBAO powder, was not added because the possible formation of Al_3Zr.[23] would confuse interpretation of the TG data.

Appropriate proportions of the starting powders were mixed and attrition-milled (Laboratory model type 01HD Szegvari Attritor System, Union Process, Akron, OH) in 400 ml of mineral spirits using 2.5 kg of high purity, 3 mm α-Al_2O_3 balls. The stirring arm rotation speed was maintained at 580 rpm.

Two hundred grams of the ABO and Al45 powders were milled for 8 h, and 100 g of Al65 powder were milled for 7 h. After milling, the Al_2O_3 balls were separated from the powder slurry using a coarse strainer and rinsed with acetone. The powder was separated from the mineral spirits and acetone by vacuum filtration. The resulting filter cake was left to dry overnight in a fume hood. Once dry, the cake was ground using a mortar and pestle and passed through a 180 μm sieve.

3.2. Powder morphology and size

The particle size distribution and average particle size were measured for each powder using a laser-scattering particle size distribution analyzer (Model LA-910, Horiba Instruments, Japan). A small quantity of powder was diluted in ethanol in a small beaker, then placed in an ultrasonic bath to break up any agglomerates. The analyzer was filled with ethanol and then the diluted powder was added until the transmittance of light through the optical cell was in the range 85–95%. The sample was continuously circulated through the optical cell, stirred, and subjected to ultrasonic vibration to maintain the particle dispersion. A measurement was taken once the particle size distribution reached a steady distribution. The average particle sizes and size distribution for the three powders, respectively, are shown in Table 2 and Fig. 3.

Table 2
Properties of RBAO powders used in experiments

Powder	Al reacted below melting point (%)	C_{Alf} (mol/cm^3)	Average particle size (μm)
30 initial vol.% Al	62.72	8.985×10^{-3}	1.635
45 initial vol.% Al	70.76	9.492×10^{-3}	1.437
65 initial vol.% Al	71.66	1.326×10^{-2}	2.628

Previous studies[2,3,7] have shown that milled aluminum particles are flake like.[23] However, for the moderate range of substrate morphologies studied in the literature, particle morphology does not appear to play a significant role in the reaction rate.

3.3. Thermogravimetric measurements

Approximately 200 mg of loose RBAO powder was used in each thermogravimetric experiment. This amount of powder was judged to be large enough weight gain to make experimental error due to the equipment insignificant, yet small enough to minimize diffusional limitations in the

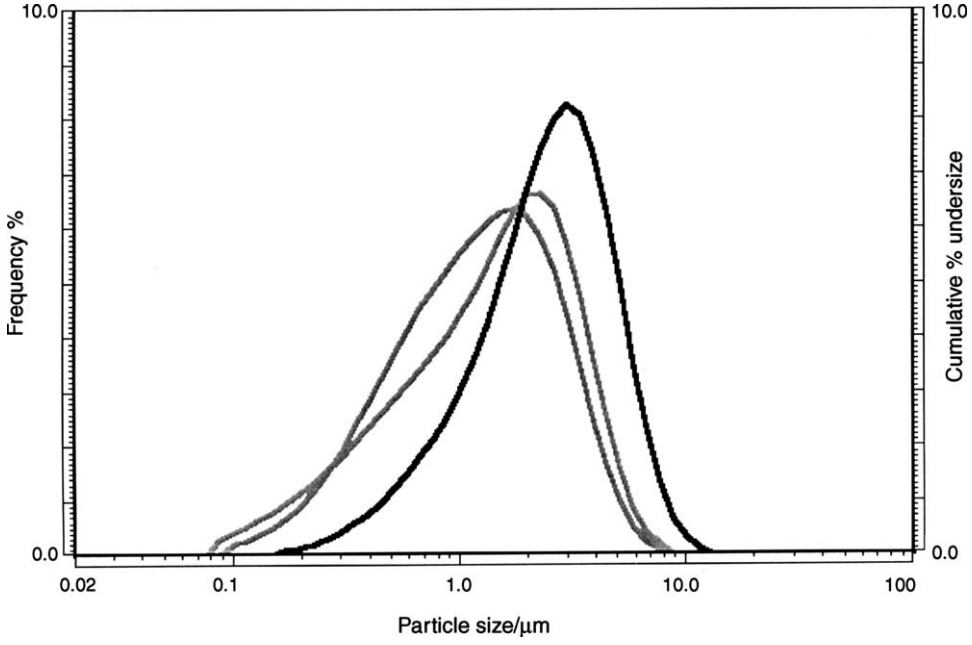

Fig. 3. Particle size distributions of RBAO powders on a volume basis.

Table 3
Post-milled powder composition

Initial powder composition	Post-milling vol.% Al	Post-milling vol.% Al_2O_3
30 initial vol.% Al	25.13	74.87
45 initial vol.% Al	34.64	65.36
65 initial vol.% Al	50.82	49.18

experiments. The degree of compaction is important since it may create diffusional limitations. However, calculations by Watson[6] for highly compacted RBAO specimens have shown that, for the rates, $R_{observerd}$, actually measured before ignition, the reaction will not be diffusionally limited.

For each experiment, the powder sample was put in an Al_2O_3 crucible, weighed, then placed in the TG analyzer (Model STA 409, Netzsch Instruments, Paoli, PA). Mixtures of oxygen and helium gas with varying compositions flowed through the TG at 50 cm^3/min. during all experiments. To ensure the desired TG atmosphere, the gas mixture was allowed to flow through the TG for 1 h before beginning each experiment. For each powder, one experiment was performed where the powder was fully reacted and the change in mass was recorded. The post-milling composition of the powders was calculated using the data from this experiment and are shown in Table 3.

Several experiments were performed on each powder with isothermal holds at various temperatures and with various gas compositions. For these experiments, the sample was heated to 20 °C below the desired temperature at a rate of 30 °C/min. and then heated to the isothermal hold temperature at a rate of l °C/min. This method of heating the sample to the isothermal hold temperature was used because it took the sample to the desired temperature in the least amount of time while avoiding any overshoot above the desired temperature. After keeping the sample at the isothermal hold temperature for 6 h, it was then cooled to 20 °C at a rate of 10 °C/min. Isothermal hold temperatures used in these experiments varied from 455 to 565 °C.

Thermal runaway occurred during the experiment with an isothermal hold temperature of 565 °C for the Al30 powder, and 535 °C for the Al45 and Al65 powders. Experiments done above these temperatures did not give useful data. For each powder (and avoiding thermal runaway), one experiment was extended from a 6 to a 12 h isothermal hold to determine the maximum oxidation below the melting point.

4. Experimental results and discussion

4.1. Effect of oxygen concentration and aluminum concentration on the reaction rate

As discussed above experiments were performed with various isothermal temperature holds for each powder with the same oxygen concentration. The weight gain versus time for the Al45 powder for varying isothermal hold temperatures (80% oxygen) are plotted in Fig. 4. It can be seen that for the higher temperatures, the reaction slows down considerably after a certain point, and then seems to stop almost completely. Calculations, however, show that there is still aluminum present at this point. Experiments performed at the highest temperature (without a runaway reaction) with a longer isothermal hold period showed that only between 70 and 80% of the total aluminum in the sample would react below the melting point. The maximum amount of aluminum that could react below the melting point was slightly different for each powder and complete conversion could only be achieved by raising the temperature above the melting point. The percentage of aluminum reacted below the melting point, the concentration of aluminum left, and the average particle size for each powder are given in Table 2.

Defining the conversion a as the aluminum reacted divided by the total amount of aluminum that will react below the melting point, the data were fit to the equation:

$$kt = -\ln(1-\alpha) \tag{3}$$

Plots of $-\ln(1-\alpha)$ versus time up to 85% conversion for the Al45 powder at various temperatures are shown in Fig. 5a and b. Plots of the data for the Al30 and Al65 powders show similar results. When the isothermal temperature is reached, the time is taken as $t = 0$, however, partial reaction occurred before the isothermal temperature was reached. The amount that reacted during heating to the isothermal temperature depended on the powder and temperature. This accounts for the varying initial points for each experiment. Beyond about 85% conversion, the reaction slowed down considerably. It seems likely that at this point, there was a change in the mechanism controlling the reaction. The reasonable fit of the experimental data in plots of $-\ln(1-\alpha)$ versus time to a straight line up to 85% conversion suggests that during this period the reaction rate was first order with respect to the amount of aluminum left in the sample. This is a purely experimental observation which has been clearly seen when taking most weight gain data in the literature.[11–15,17,18] and replotting them in terms of ($kt = -\ln(1-\alpha)$) Note that in Fig. 4a and b, the small variations in the degree of conversion at zero time arise due to corresponding differences in heat-up period prior to reaching the isothermal test temperature.

The oxygen concentration was varied in several experiments using the same powder and the same isothermal temperature. The results of experiments done on the Al30 powder at 505 °C with varying oxygen concentration are displayed in Fig. 6. The small variation between the curves shows that the effect of the oxygen concentration is negligible. This is consistent with the observations of other investigators.[11]

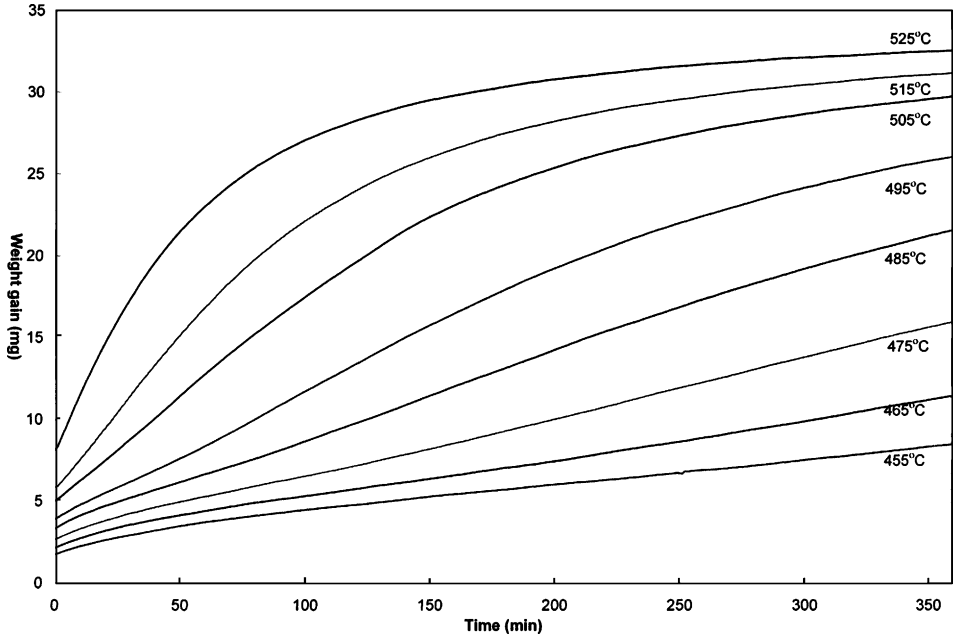

Fig. 4. Weight gain curves at various temperatures for 45 initial vol.% Al powder with oxygen concentration of 80%.

4.2. Effect of temperature

An Arrhenius plot of the rate coefficients k for the three powder compositions is shown in Fig. 7. The figure shows the Arrhenius equation ($k = k_0 \exp(-E/RT)$) to be a good approximation of the temperature dependence. All the fitted lines for each powder have approximately the same slope, independent of powder composition. The difference in the k values is a factor of about 3.4, which is not large for kinetic constants. The values of the activation energy, E, and the Arrhenius constant, k_0 that were determined from the data, as well as the average of each of these values, are shown in Table 4.

4.3. Effect of particle size

The average particle sizes of the powders are shown in Table 2, and the particle size distributions of the powders on a volume basis are shown in Fig. 3. The particle size distributions are fairly narrow with a minimum particle size of about 0.1 μm and a maximum particle size of about 11 μm. The ABO and Al45 aluminum powders have average particle sizes that are close in value, but rate coefficients and reaction rates that differ most. This is shown in Fig. 7. It also shows that the Al65 powder, which has the largest average particle size of the three powders, has a rate coefficient in between that of the other powders. This indicates that, in the limited range of particle sizes studied, particle size does not correlate with oxidation rates between 455 and 555 °C.

Table 4
Activation energies and Arrhenius constants for RBAO powders

Powder	Activation energy (kJ/mol)	Arrhenius constant (s^{-1})
30 initial vol.% Al	226	8.55×10^{10}
45 initial vol.% Al	215	2.88×10^{10}
65 initial vol.% Al	225	1.08×10^{11}
Average	222	7.41×10^{10}

4.4. Comparison of experimental data with reaction mechanisms in the literature

There exist several reaction mechanisms (with related kinetics equations) for the oxidation of aluminum that might explain the observed RBAO powder oxidation behavior.[5,11–13,16,17,22] The experimental data obtained in the present study were compared with each mechanism to check for consistency.

It has already been established that at temperatures above 450 °C the data cannot be represented by a simple parabolic equation, as done by Cabrera and Mott[22] at lower temperatures. An extension of the parabolic model to spherical particles that assumes aluminum diffusion across the oxide layer and accounts for the change in the particle size was used by Wu et al.[5] to describe the reaction kinetics of RBAO powder. At 540 °C, however, their experimental data deviated significantly from their model. It was speculated that the deviation was due to the presence of a particle size distribution and the variation of the gradient of chemical potential of the diffusing oxygen with conversion.

A more detailed analysis was advanced by Beck et al.[17] Previous investigations of the oxidation behavior of aluminum suggested that the deviation from parabolic kinetics around 450 °C was due to a change in mechanism, from diffu-

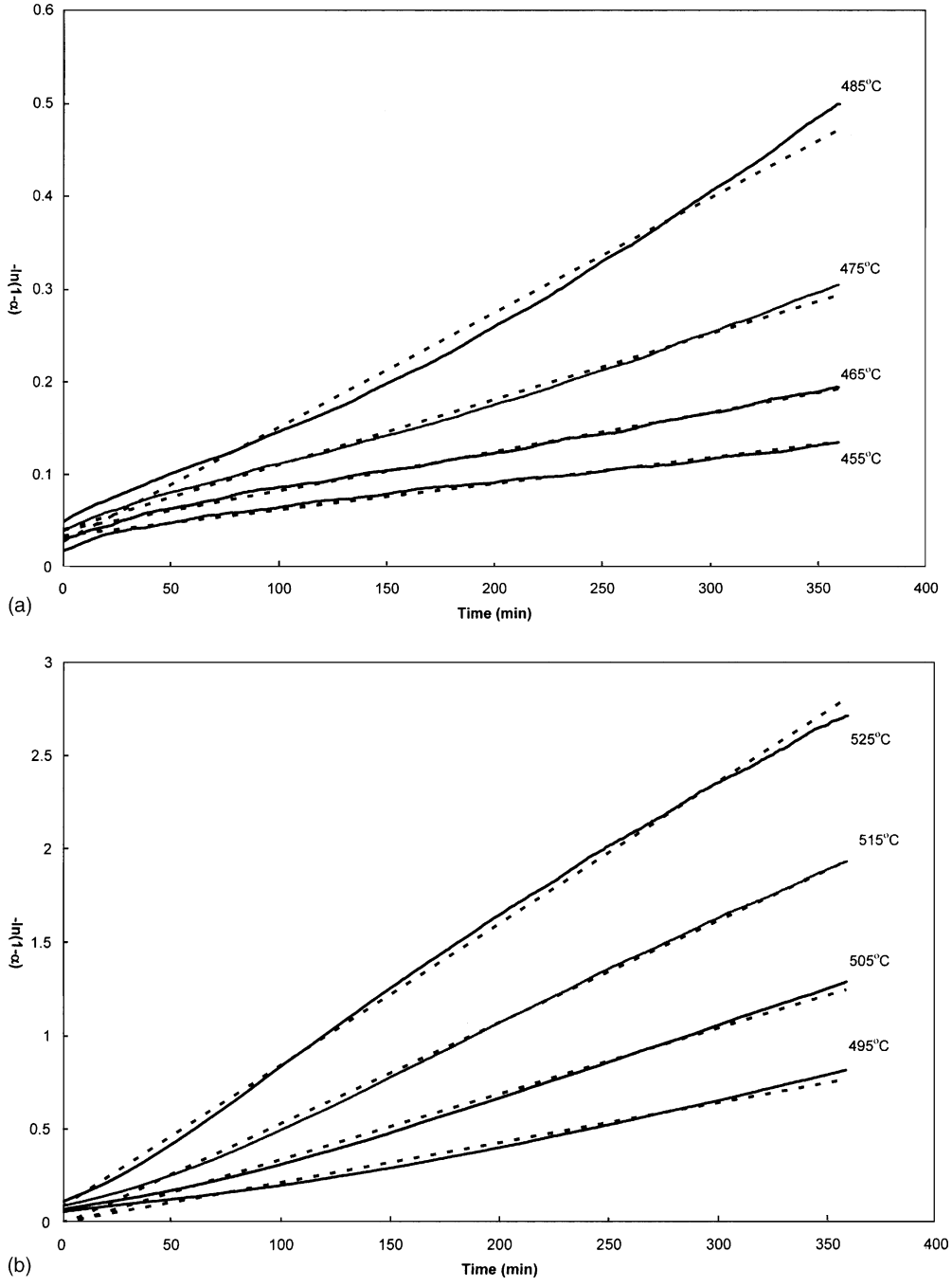

Fig. 5. (a) Fit of experimental data to first order dependence on the concentration of aluminum for 45 initial vol.% Al powder at 455, 465, 475 and 485 °C. (b) Fit of experimental data to first order dependence on the concentration of aluminum for 45 initial vol.% Al powder at 495, 505, 515, and 525 °C.

sion across an amorphous layer to a change in structure by either crystallization of the amorphous layer, or nucleation and growth of crystalline alumina, but no equations describing the kinetics were proposed.[11–13,16] Beck et al.[17] found that at temperatures between 450 and 575 °C nucleation and growth of crystalline alumina controlled the oxidation of aluminum after an initial period of parabolic growth and proceeded until the crystals ceased growth. The equation describing the crystalline growth based on uniformly expanding cylinders of constant height that nucleate instantaneously at random positions is:

$$W_c = \rho\delta[1 - \exp(-\pi v^2 \Omega t^2)] \quad (4)$$

where W_c is the weight of crystals grown on unit area; ρ, density of the crystalline alumina; δ, thickness of the crystals; v, radial velocity of growth; Ω, nucleation density, and t, time. To this value he added the rate given by the parabolic model. The model, however, contains three parameters that were adjusted at each temperature to fit the weight gain data. There are also unexplained discontinuities in the parabolic

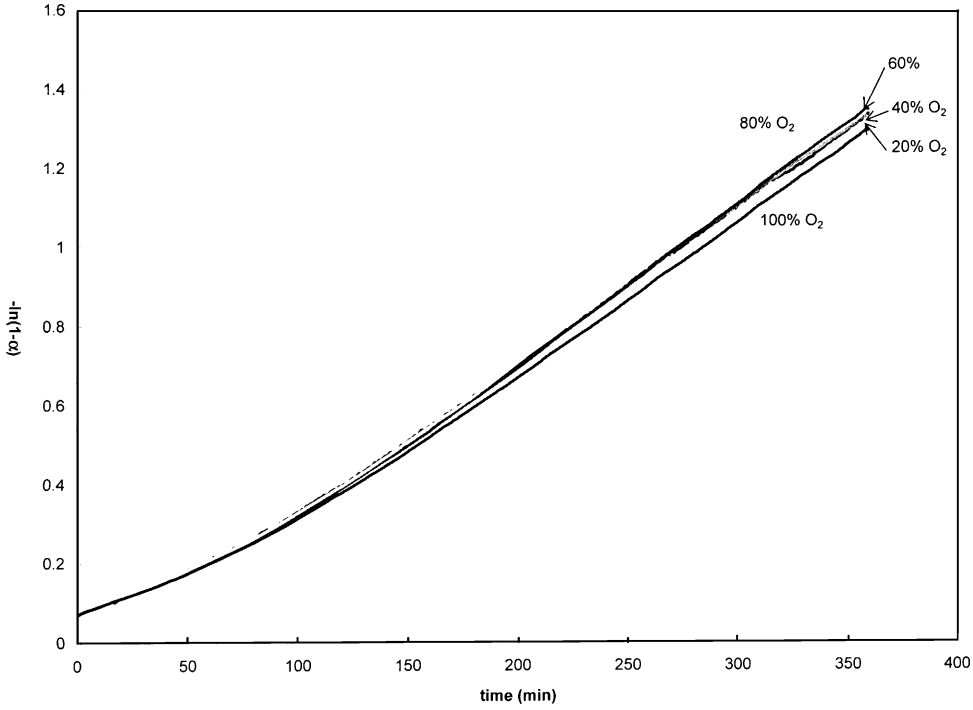

Fig. 6. Weight gain curves with various oxygen concentrations for 30 initial vol.% Al powder at 505 °C.

growth rates. Fig. 10a and b show that the first order model fits the data well. Additionally, as discussed below a single activation energy can be used to accommodate the temperature dependence.

Suvaci et al.[18] attempted to use this model to predict the oxidation rate in RBAO powder with limited success. While this may indicate that the nucleation and growth of the crystalline alumina occurred by a different mechanism in the RBAO powder than on thin, flat aluminum samples, the similarity of the shape of the weight gain curves from Beck et al.[17] and this study suggested that the mechanisms controlling the crystalline growth were the same. In spite of the number of fitting parameters available (parabolic growth rate constant, crystal linear growth rate, radial growth rate, thickness of alumina layer and nucleation density) the representation of the weight gain curves was limited to the low conversion region

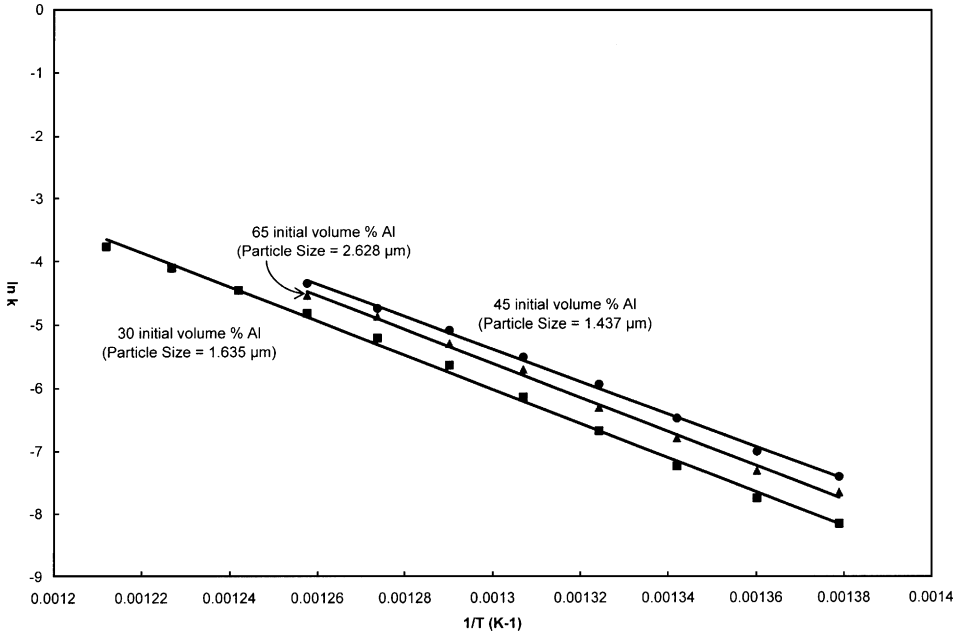

Fig. 7. Arrhenius plot of rate coefficients for various powders.

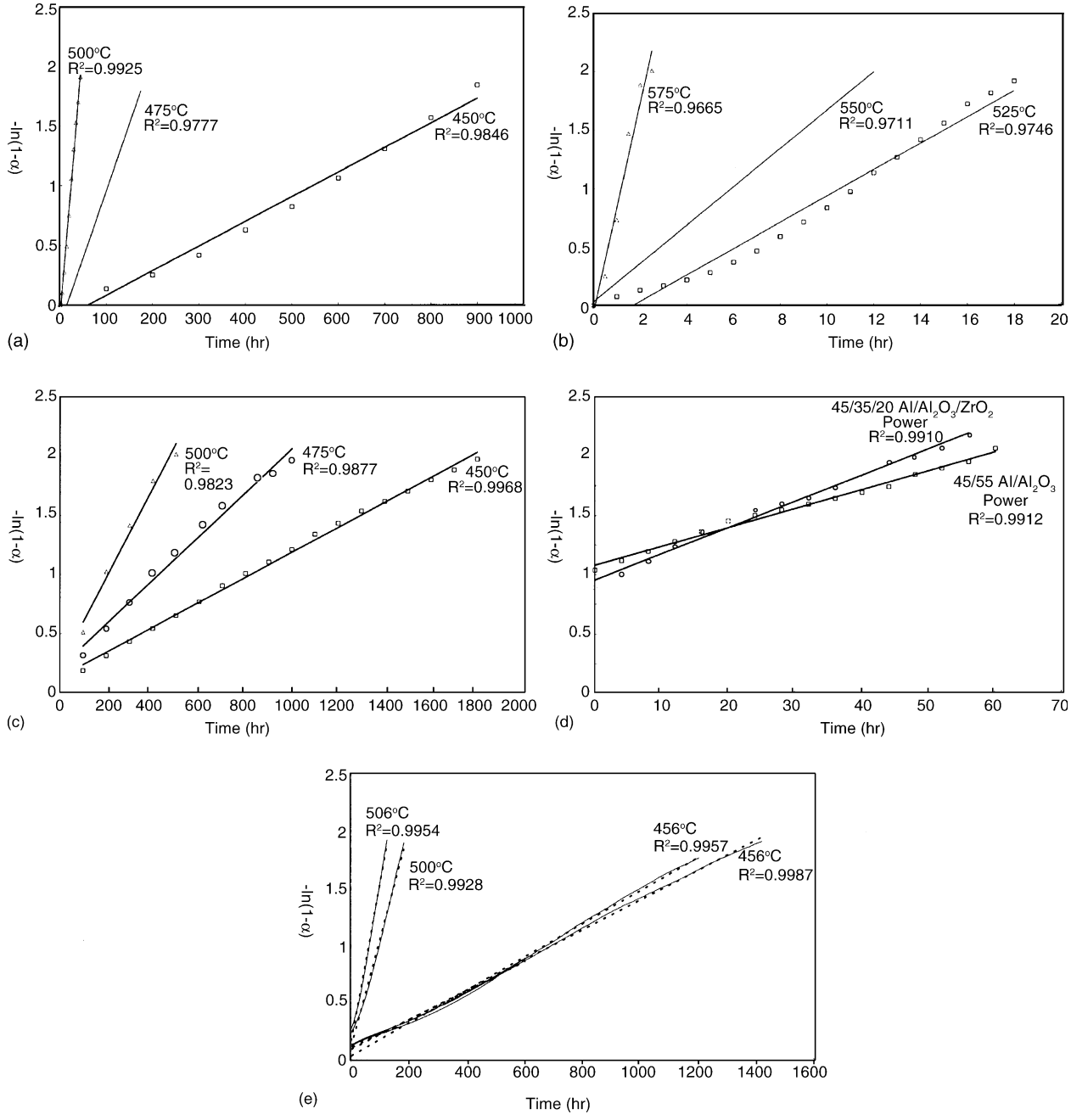

Fig. 8. (a) Fit of experimental data from Beck et al. to first order dependence on the concentration of aluminum at 450, 475, and 500 °C. (b) Fit of experimental data from Beck et al. to first order dependence on the concentration of aluminum at 525, 550, and 575 °C. (c) Fit of experimental data from Suvaci et al. to first order dependence on the concentration of aluminium at 450, 475, and 500 °C. (d) Fit of experimental data from Wu et al. to first order dependence on the concentration of aluminum at 540 °C for powders of different composition. (e) Fit of experimental data from Gaus to first order dependence on the concentration of aluminum at 456, 500, and 506 °C.

of the process, with significant deviations at higher conversions.

It should be noted that most past studies have shown a brief initial region of rapidly decreasing reaction rates that were not seen in this work. This may be due to the period of heating at the beginning during which partial oxidation occurred. However, the initial region of decreasing reaction rate found in most studies corresponded to very small conversions, so the lack of observation of this region was not significant for the purpose of this study.

4.5. Consistency of literature data with first order reaction kinetics

The difficulties encountered by previous investigators in representing the oxidation rates were discussed in the

Table 5
Activation energies and Arrhenius constants of data fitting a first order equation for various studies

Data source	Temperature range (°C)	Activation energy (kJ/mol)	Arrhenius constant (s^{-1})
Beck et al.[17]	450–575	230	1.84×10^{12}
Suvaci et al.[18]	450–500	119	6.31×10^{3}
This study 30 initial vol.% Al	455–555	226	8.55×10^{10}
This study 45 initial vol.% Al	455–525	215	2.88×10^{10}
This study 65 initial vol.% Al	455–525	225	1.08×10^{11}

previous section. The question naturally rises, therefore, is the experimental data in the literature consistent with the reaction kinetics observed in the present work? To address this point, the data from several groups were fit to the first order equation up to 85% conversion, and assuming a maximum conversion as indicated by the individual curves. The fit of the data is shown in Fig. 8a and b for Beck et al.,[17] in Fig. 8c for Suvaci et al.,[18] and in Fig. 8d for Wu et al.,[5] and in Fig. 8e for Gaus.[3] Coefficients of regression (R^2) exceed 0.99.

An Arrhenius plot with the rate coefficients found in Fig. 8a–e is shown in Fig. 9. The activation energies and Arrhenius constants determined from the figure are given in Table 5. As before, the data of Beck et al.[17] and Suvaci et al.[18] are significantly lower than the rest. Regardless, the figure shows, as stated earlier, that the reaction constants are close to those from other investigators. Measurements of the rate of oxidation of RBAO compacts were carried out by Suvaci et al.[18] for flat pellets 2.5 and 4.0 mm thick, at temperatures from 410 to 495 °C. Since the weight gain curves were very well represented by the first order kinetics model, the values of the apparent kinetic constants are also presented in Fig. 9. The data are remarkably close to the kinetic constants obtained in this work for loose powders and they fall in a trend line that shows the same activation energy as the loose powder measurements. Additionally, the data fit extend to temperatures as low a 410 °C considerably extending the range of temperature for which the model can be applied. Some of the data at high temperature show a rapid initial rate with a sudden slowdown at low conversions. It is likely that the data correspond to runaway conditions and were not included in the analysis. In several studies, reported in the literature, the point of maximum conversion was not reached hence the first order equation could not be fit to the data. However, for low conversions, the first order equation can be approximated by a linear equation of the form

$$\alpha = kt \tag{5}$$

where α is the conversion, k is the rate coefficient, and t is time. An Arrhenius plot of the rate coefficients, as rate of weight gain per unit area, extracted from data in the linear region of the weight gain curve for several oxidation studies (including the current work) is shown in Fig. 10. The figure contains rate coefficients from data collected by Gulbransen and Wysong[11] (one sample), Smeltzer[15] (two differently

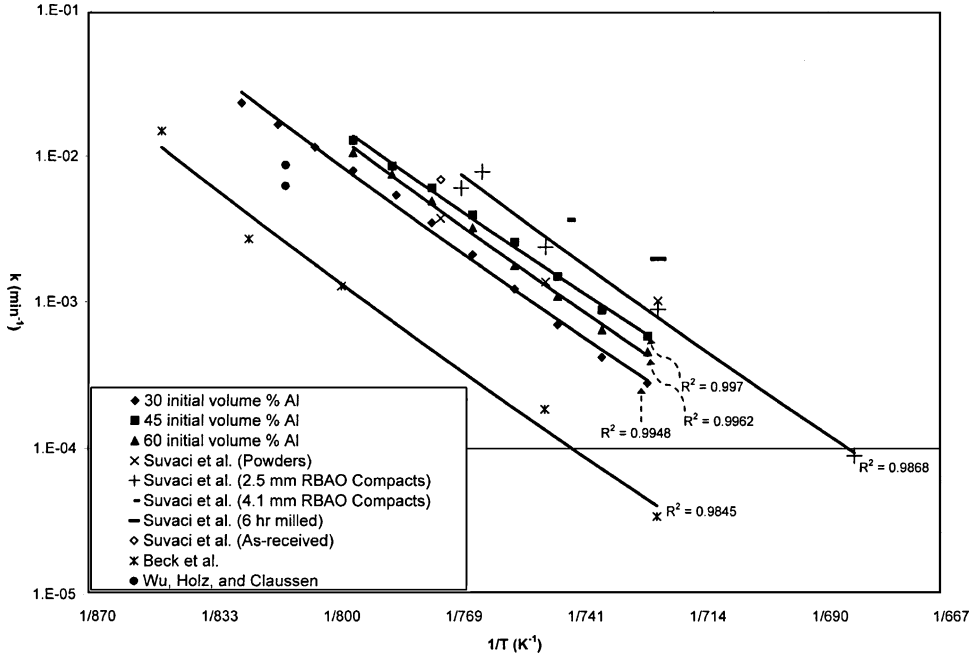

Fig. 9. Arrhenius plot of rate coefficients for experimental data from this study and various other studies.

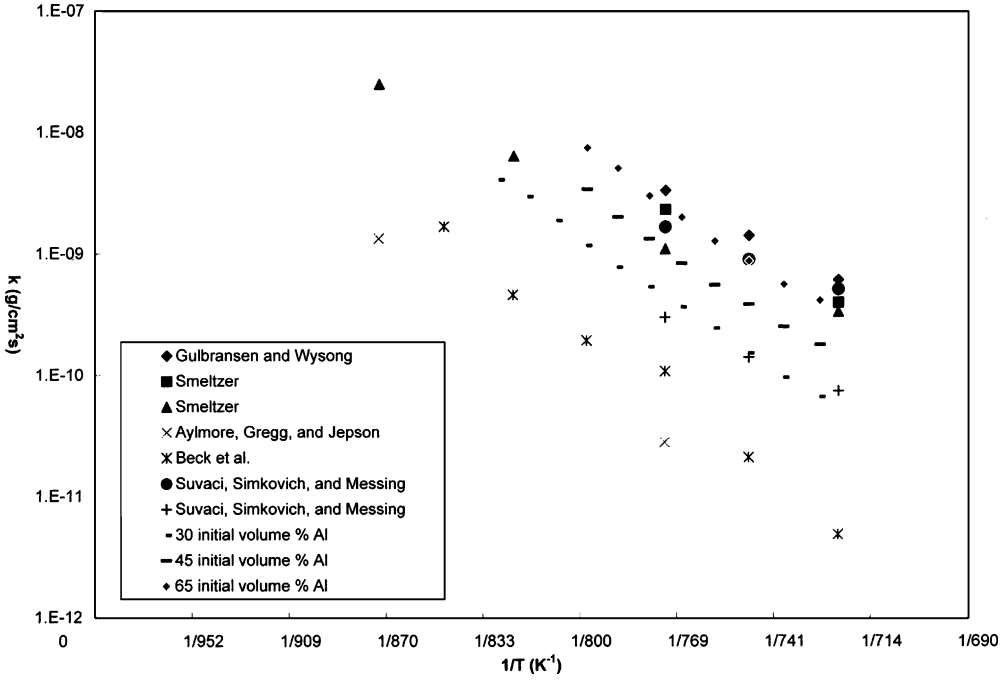

Fig. 10. Arrhenius plot of rate coefficients from data fitting linear equation studies.

prepared samples), Aylmore et al.[13] (one sample), Beck et al.[17] (one sample), Suvaci et al.[18] (two differently prepared samples), and this study (the powders containing 30, 45, and 65 initial vol.% Al). The activation energies and Arrhenius constants determined from the data used in Fig. 10 is are tabulated in Table 6.

Despite the variations in the activation energies and Arrhenius constants for each set of data, the values of the rate coefficients in Fig. 10 are similar for all the studies; with the exception of data from Beck and Aylmore, the overall slope is the same. From this, a single activation energy and Arrhenius constant can be determined if all the data are considered together. This shows that the behavior of the oxidation of aluminum is similar for flat samples and powders with various preparation techniques and that the equation(s) describing the kinetics at various temperatures should be the same for all the studies. We acknowledge that this is purely a phenomenological description, and the reaction mechanisms are still obscure. Nonetheless, it is significant that a relatively simple kinetic model has applicability over a broad range of data in the literature.

An attempt was made to fit the experimental data above 85% conversion from this study to an equation that might correlate to a change in mechanism. However, no equation was found to fit this data, and it is difficult to suggest a mechanism to explain the behavior in this region.

4.6. Applications of kinetics equations to prior reaction bonding results

In previous work, Gaus obtained curves for several runs on compacted RBAO samples with isothermal temperature holds at different temperatures for different lengths of time. Fig. 11 shows a comparison between the weight gain curves obtained by Gaus[3] and the weight gain predicted by the first order equation using the average activation energy and

Table 6
Activation energies and Arrhenius constants of data fitting a linear rate law for various studies

Data source	Temperature range (°C)	Activation energy (kJ/mol)	Arrhenius constant (g/cm^2 s)
Gulbransen and Wysong[11]	450–500	158	1.5×10^2
Smeltzer[15]	450–600	164	2.8×10^2
		153	3.4×10^1
Aylmore et al.[13]	500–650	217	1.3×10^4
Beck et al.[17]	450–575	228	1.8×10^5
Suvaci et al.[18]	450–575	111	4.2×10^{-2}
		128	1.8×10^{-1}
This study	455–555	209	5.6×10^4
		202	5.0×10^4
		203	1.4×10^5

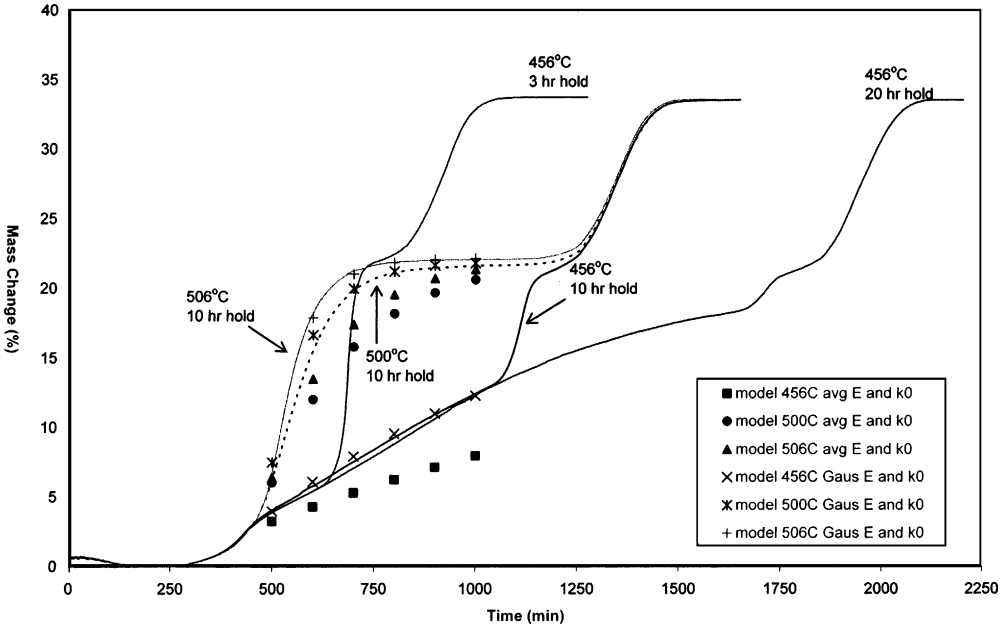

Fig. 11. Experimental (continuous lines) and predicted weight gains at various temperatures and isothermal hold lengths using different first order kinetics.

Arrhenius constant determined in this study. The corresponding data calculated using the first order equation and an activation energy and Arrhenius constant derived from Gaus's own work are also included. The determined activation energy and Arrhenius constant predict the weight gain curve very well. The prediction of weight gain using the average activation energy and Arrhenius constant determined in this study is somewhat lower than the actual weight gain but still very reasonable. It is obvious that some variation between RBAO powders can be expected, but the average activation energy and Arrhenius constant values will provide a useful estimate of weight gain and noticing that there are always variations between powders.

Watson[6] performed experiments on samples of compacted RBAO where a maximum reaction rate was set to avoid both diffusion control of the reaction and ignition.[6] Avoiding diffusion control and ignition prevents the development of thermal and chemical stresses which cause sample cracking.

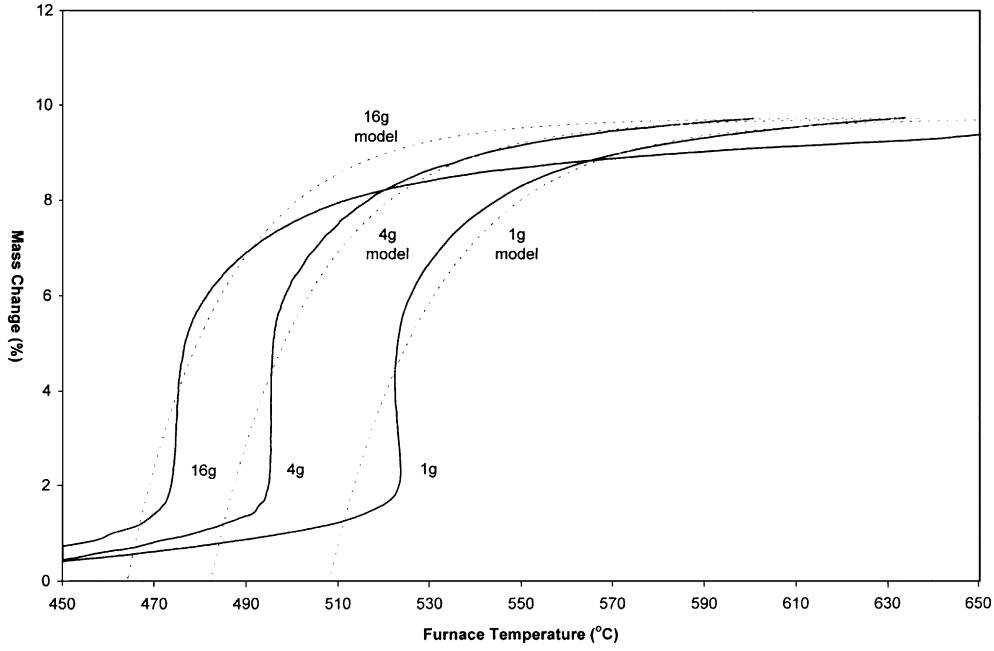

Fig. 12. Experimental weight gain vs. temperature curves for 1 g, 4 g, and 16 g samples from Watson (continuous lines) and as predicted by first-order equation (dotted lines).

In his experiments, the temperature would increase at a rate of 5 °C/min if the reaction rate was below a maximum rate, chosen to prevent both ignition and concentration gradients. When the reaction rate reached the maximum set value, the temperature would stay the same or increase slowly to keep the reaction rate at the set value. Weight gain versus temperature curves are plotted in Fig. 12. It shows data for several samples from Watson in the region where the reaction rate is approximately constant at the maximum set value and shows the temperature predicted from the first order equation for the mass and set reaction rate of each sample. The predicted curves start at the minimum temperature that will give the desired rate for the unconverted sample. The predicted temperatures and the experimental values of the sample temperatures match very well.

5. Conclusions

In the temperature range 455–555 °C, the reaction kinetics for the oxidation of RBAO powders was observed to be first order with respect to the concentration of aluminum, and zero order with respect to the concentration of oxygen. The kinetics were also found to have an Arrhenius dependence on temperature with an activation energy of 222 kJ/mol and an Arrhenius constant in the range 2.88×10^{10} to $1.08 \times 10^{11}\ s^{-1}$. A survey of the literature revealed that the experimental data from a broad range of studies were also consistent with the aforementioned kinetics model put forward. Further, the proposed correlation is simpler than the multiple regions and mechanisms presented previously. Over the small range of average Al/Al_2O_3 particle sizes examined, there was little influence of average particle size on oxidation kinetics. The kinetics presented will be useful to predict the reaction behavior of RBAO powder compacts as long as diffusional effects are not important, and ignition is avoided.

References

1. Claussen, N., Le, T. and Wu, S., Low-shrinkage reaction-bonded alumina. *Eur. Ceram. Soc.*, 1989, **5**, 29–35.
2. Gaus, S. P., Harmer, M. P., Chan, H. M. and Caram, H. S., Controlled firing of reaction-bonded aluminum oxide (RBAO) ceramics: Part I. Continuum model predictions. *Am. Ceram. Soc.*, 1999, **82**, 897–908.
3. Gaus, S. P., *Modeling of the Reaction-Based Processing of Aluminum Oxide (RBAO) and Alumina–Aluminide Alloys (3A)*. Ph.D. dissertation, Lehigh University, January 1998.
4. Claussen, N., Janssen, R. and Holz, D., The reaction bonding of aluminum oxide (RBAO). *Ceram. Soc. Jpn.*, 1995, **8**, 1–10.
5. Wu, S., Holz, D. and Claussen, N., Mechanisms and kinetics of reaction-bonded aluminum oxide ceramics. *Am. Ceram. Soc.*, 1993, **76**, 970–980.
6. Watson, M. J., *Ignition Phenomena and Controlled Firing of Reaction-Bonded Aluminum Oxide*. Ph.D. dissertation, Lehigh University, May 1999.
7. Gaus, S. P., Sheedy, P. M., Caram, H. S., Chan, H. M. and Harmer, M. P., Controlled firing of reaction-bonded aluminum oxide (RBAO) ceramics: Part II. Experimental results. *Am. Ceram. Soc.*, 1999, **82**, 909–915.
8. Holz, D., Wu, S., Scheppokat, S. and Claussen, N., Effect of processing parameters on phase and microstructure evolution in RBAO ceramics. *Am. Ceram. Soc.*, 1994, **77**, 2509–2517.
9. Claussen, N., Wu, S. and Holz, D., Reaction bonding of aluminum oxide (RBAO) composites: processing, reaction mechanisms and properties. *Eur. Ceram. Soc.*, 1994, **14**, 97–109.
10. Claussen, N., Travitzky, N. A. and Wu, S., Tailoring of reaction-bonded Al_2O_3 (RBAO) ceramics. *Ceram. Eng. Sci. Proc.*, 1990, **11**, 806–820.
11. Gulbrasen, E. A. and Wysong, W. S., Thin oxide films on aluminum. *Phys. Colloid Chem.*, 1947, **51**, 1087–1103.
12. Aumann, C. E., Skofronick, G. L. and Martin, J. A., Oxidation behavior of aluminum nanopowders. *Vac. Sci. Tech.*, 1995, **13**, 1178–1183.
13. Aylmore, D. W., Gregg, S. J. and Jepson, W. B., The oxidation of aluminum in dry oxygen in the temperature range 400–650 °C. *J. Inst. Metals*, 1960, **88**, 205–208.
14. Cochran, C. N. and Sleppy, W. C., Oxidation of high-purity aluminum and 5052 aluminum–magnesium alloy at elevated temperatures. *J. Electrochem. Soc.*, 1961, **108**, 322–327.
15. Smeltzer, W. W., Oxidation of aluminum in the temperature range 400–600 °C. *J. Electrochem. Soc.*, 1956, **103**, 209–214.
16. Dignam, M. J., Oxide films on aluminium. II. Kinetics of formation in oxygen. *J. Electrochem. Soc.*, 1962, **109**, 192–198.
17. Beck, A. F., Heine, M. A., Caule, E. J. and Pryor, M., Kinetics of the oxidation of Al in oxygen at high temperatures. *Con. Sci.*, 1967, **7**, 1–22.
18. Suvaci, E., Simkovich, G. and Messing, G. L., The reaction-bonded aluminum oxide process: I. The effect of attrition milling on the solid-state oxidation of aluminum powder. *J. Am. Ceram. Soc.*, 2000, **83**, 299–305.
19. Thomas, K. and Roberts, M. W., Direct observation in the electron microscope of oxide layers on aluminum. *J. Appl. Phys.*, 1961, **32**, 70–75.
20. Doherty, P. E. and Davis, R. S., Direct observation of aluminum single crystal surfaces. *J. Appl. Phys.*, 1963, **34**, 619–628.
21. Rode, H., Hlavacek, V., Viljoen, H. and Gatica, J. E., Combustion of metallic powders: a phenomenological model for the initiation of combustion. *Combust. Sci. Technol.*, 1992, **88**, 153–175.
22. Cabrera, N. and Mott, N. F., Theory of oxidation of metals. *Rep. Prog. Phys.*, 1949, **12**, 163–184.
23. Sheedy, P. M., Caram, H. S., Chan, H. M. and Harmer, M. P., Effects of ZrO2 on the reaction bonding of aluminum oxide. *J. Am. Ceram. Soc.*, 2001, **84**(5), 986–990.